Structures for d^0 ML_6 and ML_5 Complexes

Sung Kwon Kang,[1a] Huang Tang,[1b] and Thomas A. Albright*,[1b]

Contribution from the Departments of Chemistry, University of Houston, Texas 77204-5641, and Chungnam National University, Daejeon, 301-764 Korea. *Received September 8, 1992*

Abstract: A second-order Jahn-Teller argument is given to explain why certain d^0 ML_6 and ML_5 molecules will have geometries different from the octahedron and the trigonal bipyramid, respectively, as given by the VSEPR rules. Ab initio molecular orbital calculations were used to explore the potential energy surface for a variety of molecules. In the CrH_6 system, 20 stationary points were located and six were selected for study using a number of basis sets and electron correlation methods. The global minimum appears to be a C_{3v} $(\eta^2\text{-}H_2)_3Cr$ isomer which QCISD(T) calculations put at being 165 kcal/mol more stable than the octahedral (O_h) one. However, two other geometries of C_{3v} symmetry, one greatly distorted from the octahedron and the other distorted from a trigonal prism, are also computed to lie at a low energy and could possibly become the ground state at a higher computational level. For WH_6, nine stationary points were located and either a C_{3v} distorted trigonal prism or a novel C_{5v} pentagonal pyramid was found to be 142 kcal/mol (QCISD(T)) more stable than O_h. In TaH_5 and VH_5, the square pyramid (C_{4v}) was found to be 20 and 27 kcal/mol, respectively, more stable than the trigonal bipyramid (D_{3h}). A new mechanism for apical-basal exchange in these molecules is proposed, wherein two trans basal hydrogens pivot around an axis orthogonal to the plane defined by the apical atom, Ta, and two remaining basal atoms. For WMe_6 and $TaMe_5$, the ground-state structures are in very good agreement with gas-phase electron diffraction results. The trigonal prism is computed to be 83 kcal/mol more stable than the octahedron for WMe_6 and the square pyramid 7.7 kcal/mol more stable than the trigonal bipyramid at the MP2 level. For WF_6, CrF_6, VF_5, and $TaCl_5$, VSEPR anticipated geometries were found to be more stable than other structural alternatives.

Introduction

The valence shell electron pair repulsion (VSEPR) model[2] occupies a central position in structural chemistry. It has wide applicability, simplicity, and much predictive success. There have been occasional concerns about its theoretical underpinnings or quantitative details;[2c,3] however, we are aware of only three general instances where the VSEPR model does not yield correct results in qualitative terms. Reed, Schleyer, and Janoschek[4] found C_{2v} structures to be more stable than T_d in the four-electron-pair ALi_4 molecules, where A = Si, Ge, and Sn. Marsden has also identified non-VSEPR structures for PLi_5, SLi_4 and SLi_6.[5] In these cases, attractive interactions between the Li atoms have been highlighted. The second instance originates from the so-called "inert-pair effect". For example, BrF_6^-, with seven electron pairs, was found to possess an octahedral rather than a capped octahedral geometry.[6] Likewise, XeF_8^{2-}, with nine electron pairs, is square antiprismatic rather than a tricapped trigonal prism.[7] The final group contains certain d^0 ML_n transition-metal complexes, which are the subject of this manuscript. The central thesis here is that in special instances a small HOMO-LUMO gap will exist for a d^0 ML_n complex at the VSEPR mandated geometry. This signals a potential second-order Jahn-Teller distortion.[8] The distortion will serve to mix the LUMO into the HOMO, stabilizing the latter. The HOMO-LUMO gap must be small since the stabilization afforded to the HOMO is inversely dependent upon this gap. There will always be other lower-lying, filled orbitals which are destabilized along the distortion mode, and these serve as a braking force for the distortion. In a practical sense, a nonbonding metal d orbital is required for a low-lying LUMO. Furthermore, the surrounding ligands should possess little or no π-donating capacity which would serve to destabilize the LUMO. Likewise, the metal should not be too electropositive. A high-lying HOMO is obtained when the surrounding ligands are strong σ-donors. The metal-ligand bond should be reasonably covalent. An extreme ionic case simply reduces to a point charge on a sphere problem, for which a solution is given by the VSEPR approach. Lastly, for obvious steric reasons, the ligands must not be bulky. Previously, calculations revealed that a number of the two-electron-pair AX_2 molecules, where A = Sr and Ba and X = H, F, Cl, Br, and I, are bent rather than linear.[9] The three-electron-pair molecules ScH_3, TiH_3^+, and $TiMe_3^+$ were computed to be pyramidal rather than planar.[10,11] In both cases, d orbital occupation increased upon distortion to the non-VSEPR geometry. This is precisely what one would expect from second-order Jahn-Teller arguments. Our original interest in this area was derived from the idea[12] that several d^0 ML_6 complexes[13] were distorted not by the formation of an agostic bond which occupied a seventh coordination site but rather by an intrinsic potential to distort from the octahedron. We initially[14] examined octahedral versus trigonal prismatic geometries for TiH_6^{2-}, CrH_6, and CrF_6. In this publication, the full potential energy surfaces shall be examined for a variety of d^0 ML_6 and ML_5 molecules using ab initio molecular orbital theory.

Computational Methods

All ab initio molecular orbital computations were carried out with the GAUSSIAN 82,[15] GAUSSIAN 90,[16] and GAMESS[17] packages. Three

(1) (a) Chungnam National University. (b) University of Houston.

(2) (a) Gillespie, R. J.; Nyholm, R. S. *Q. Rev. Chem. Soc.* **1957**, *11*, 339. (b) Gillespie, R. J. *Molecular Geometry*; van Nostrand-Reinhold: London, 1972. (c) Gillespie, R. J.; Hargittai, I. *The VSEPR Model of Molecular Geometry*; Allyan and Bacon: Boston, 1991.

(3) See, for example: Hall, M. B. *Inorg. Chem.* **1978**, *17*, 2261. Burdett, J. K.; Fässler, T. F. *Ibid.* **1991**, *30*, 2859. Baird, N. C. *Ibid.* **1989**, *28*, 1224. Gillespie, R. J. *Can. J. Chem.* **1992**, *70*, 742.

(4) Reed, A. E.; Schleyer, P. v. R.; Janoschek, R. *J. Am. Chem. Soc.* **1991**, *113*, 1885.

(5) Marsden, C. J. *J. Chem. Soc., Chem. Commun.* **1989**, 1356.

(6) (a) Mahjoub, A. R.; Hoser, A.; Fuchs, J.; Seppelt, K. *Angew. Chem.* **1989**, *101*, 1528; *Angew. Chem., Int. Ed. Engl.* **1989**, *28*, 1526. (b) For an excellent survey and theoretical analysis, see: Wheeler, R. A.; Pavankumar, P. N. V. *J. Am. Chem. Soc.* **1992**, *114*, 4776.

(7) Peterson, S. W.; Holloway, J. H.; Coyle, B. A.; Williams, J. M. *Science* **1971**, *173*, 1238.

(8) Albright, T. A.; Burdett, J. K.; Whangbo, M.-H. *Orbital Interactions in Chemistry*; Wiley: New York, 1985.

(9) (a) Kaupp, M.; Schleyer, P. v. R.; Stoll, H.; Preuss, H. *J. Am. Chem. Soc.* **1991**, *113*, 6012. (b) Kaupp, M.; Schleyer, P. v. R.; Stoll, H.; Preuss, H. *J. Chem. Phys.* **1991**, *94*, 1360. (c) See also: Kaupp, M.; Schleyer, P. v. R. *J. Phys. Chem.* **1992**, *96*, 7316. Kaupp, M.; Charkin, O. P.; Schleyer, P. v. R. *Organometallics* **1992**, *11*, 2765.

(10) Jolly, C. A.; Marynick, D. S. *Inorg. Chem.* **1989**, *28*, 2893.

(11) Musaev, D. G.; Charkin, O. P. *Koordinat. Khim.* **1989**, *15*, 161.

(12) Demolliens, A.; Jean, Y.; Eisenstein, O. *Organometallics* **1986**, *5*, 1457.

(13) For other computational studies on these molecules, see: Koga, N.; Obara, S.; Morokuma, K. *J. Am. Chem. Soc.* **1984**, *106*, 4625; *J. Organomet. Chem.* **1984**, *270*, C33.

(14) Kang, S. K.; Albright, T. A.; Eisenstein, P. *Inorg. Chem.* **1989**, *28*, 1611.

0002-7863/93/1515-1971$04.00/0

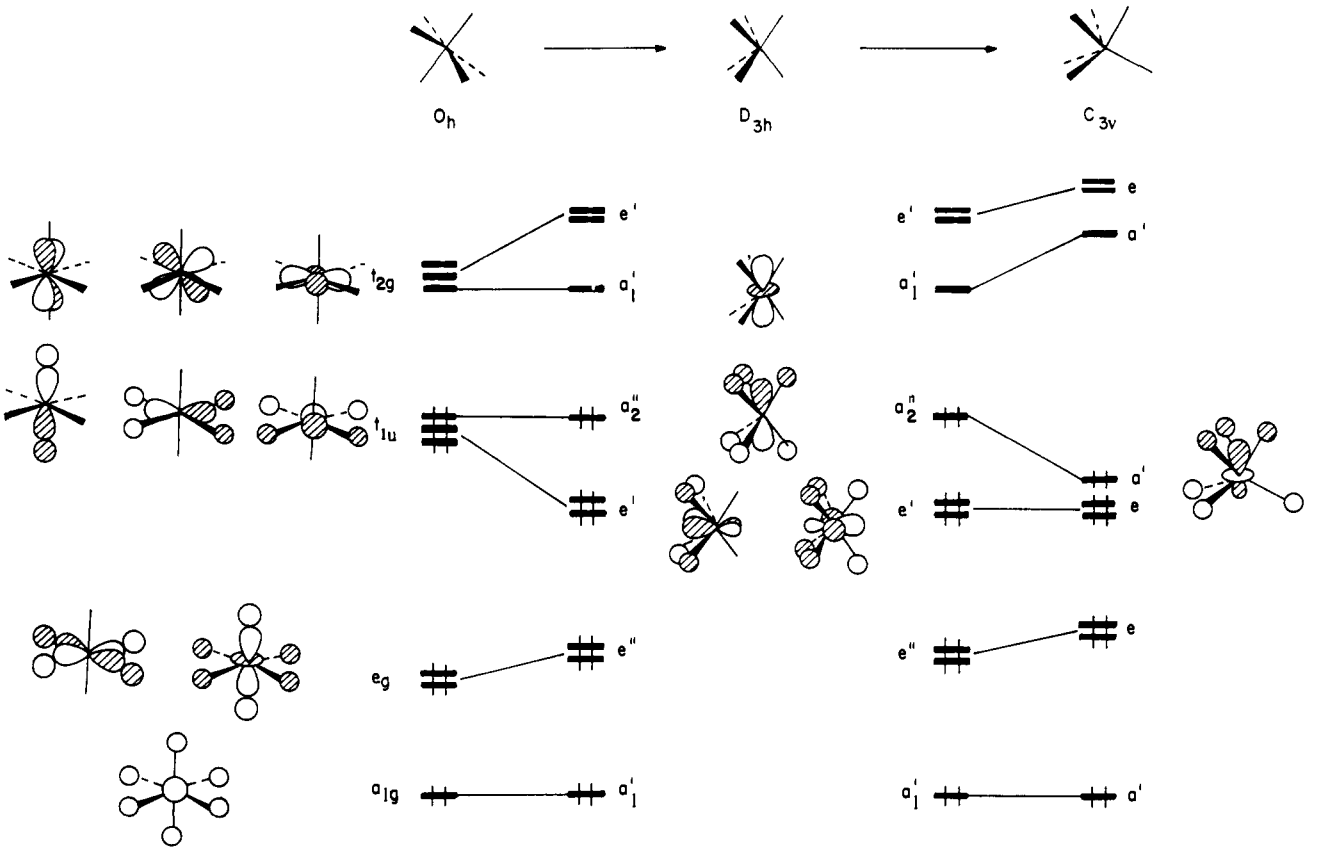

Figure 1. Orbital correlation diagram for the distortion of a d^0 MH_6 molecule from the O_h to D_{3h} to C_{3v} geometries.

all-electron basis sets were used for the chromium and vanadium complexes. The first, referred to as basis I, was of the form (4333/433/31) for the metal atoms and has been described elsewhere.[14] Basically, it is of double-ζ quality for the metal d region and single-ζ elsewhere. Standard 4-31G basis sets for hydrogen and fluorine[18] were used in conjunction with it. Basis II was derived from the Wachters expansion of the form (62111131/511231/411) for the metal atoms.[14] Here the metal d orbitals are triple-ζ and all others are double-ζ. The hydrogens employed a 6-311G** basis,[19] and the Dunning [5s/3p] basis[20] was used for fluorine. In basis III an f function with an exponent of 1.0582 (for chromium)[21] was added to metal basis II, and the associated ligands used the same basis sets as those in basis II. For the tungsten and tantalum complexes, a relativistic effective core potential[22a] was used for the 1s through 4d electrons. The 5s through 6p electrons were explicitly treated with an associated double-ζ basis.[22a] We should mention that early pilot calculations on WF_6 were carried out with an effective core potential[23] that included the 5s and 5p electrons. At the octahedral geometry, the W–F distances were found to be 0.175 Å too long, and the trigonal prismatic geometry was found to be more stable than the octahedral one, contrary to experiment (vide infra). The hydrogen and fluorine 4-31G basis was again used for the ligands, and in $TaCl_5$ a standard effective core potential and associated basis[22b] were employed for Cl. For WMe_6 and $TaMe_5$, a 3-21G basis was used for carbon[24] and an STO-3G basis for hydrogen.[25]

All optimized geometries and all total energies are reported in the supplementary material. Numerical harmonic frequencies for the stationary points at the MP2 level for CrH_6, WH_6, TaH_5, and VH_5 as well as frequencies at the Hartree–Fock (HF) level for VF_5 and $TaCl_5$ are also given as supplementary material. Optimizations of CrH_6, VH_5, CrF_6, and TaH_5 were carried out at the MP2 level. The MP2 energies then correspond to all electrons being correlated. For CrH_6, WH_6, TaH_5, VH_5, $TaCl_5$, and CrF_6, an extensive study was undertaken for the effect of electron correlation on the relative stability of selected geometrical isomers. The correlated methods included full MP4,[27] MP4(SDQ) (where triple substitutions were not included), CCD[28] (coupled cluster theory with double substitutions), ST4CCD[29] (evaluation of the single and triple substitutions to fourth order using the CCD wave function), QCISD[30] (quadratic CI with single and double substitutions), and QCISD(T) (evaluation of the triple substitutions). Pilot calculations were carried out with and without the frozen core approximation using these techniques. Only very small variations in the relative energies were found. All of the energies reported are those using the frozen core approximation. This is also true for the MP2 calculations using bases II and III.

CrH_6 and WH_6 Molecules

For a ML_6 complex with a d^0 electron count at the metal, the VSEPR rules clearly stipulate the preferred geometry to be octahedral.[2] This has also been demonstrated to be the optimal one on steric grounds by several force field calculations.[31] As men-

(15) Binkley, J. S.; Frisch, M.; Raghavachari, K.; Fluder, E.; Seeger, R.; Pople, J. A. *Gaussian 82*; Carnegie-Mellon Publishing Unit: Pittsburgh, PA, 1982.

(16) Frisch, M. J.; Head-Gordon, M.; Trucks, G. W.; Foresman, J. B.; Schlegel, H. B.; Raghavachari, K.; Robb, M. A.; Binkley, J. S.; Gonzalez, C.; Defrees, D. J.; Fox, D. J.; Whiteside, R. A.; Saeger, R.; Melius, C. F.; Baker, J.; Martin, R. L.; Kahn, L. R.; Stewart, J. J. P.; Topiol, S.; Pople, J. A. *Gaussian 90*; Gaussian, Inc.: Pittsburgh, PA, 1990.

(17) Schmidt, M. W.; Baldridge, K. K.; Boatz, J. A.; Jensen, J. H.; Koeski, S.; Gordon, M. S.; Nguyen, K. A.; Windus, T. L.; Elbert, S. T. *QCPE Bull.* **1990**, *10*, 52.

(18) Ditchfield, R.; Hehre, W. A.; Pople, J. A. *J. Chem. Phys.* **1971**, *54*, 724.

(19) Krishman, R.; Binkley, J. S.; Seeger, R.; Pople, J. A. *J. Chem. Phys.* **1980**, *72*, 650.

(20) Dunning, T. H., Jr. *J. Chem. Phys.* **1970**, *53*, 2823.

(21) Stewart, R. F. *J. Chem. Phys.* **1970**, *52*, 431. Walch, S. P.; Bauschlicher, C. W., Jr. *Chem. Phys. Lett.* **1984**, *105*, 171.

(22) (a) Hay, P. J.; Wadt, W. R. *J. Chem. Phys.* **1985**, *82*, 299. (b) Wadt, W. R.; Hay, P. J. *Ibid.* **1985**, *82*, 284.

(23) (a) Hay, P. J.; Wadt, W. R. *J. Chem. Phys.* **1985**, *82*, 270. (b) Other workers have noted related problems, see: Pacios, L. F.; Olcina, V. B. *J. Chem. Phys.* **1991**, *95*, 441 and references therein.

(24) Binkley, J. S.; Pople, J. A.; Hehre, W. J. *J. Am. Chem. Soc.* **1980**, *102*, 939.

(25) Hehre, W. J.; Stewart, R. F.; Pople, J. A. *J. Chem. Phys.* **1969**, *51*, 2657.

(26) Möller, C.; Plesset, M. S. *Phys. Rev.* **1934**, *46*, 618.

(27) Krishman, R.; Frisch, M. J.; Pople, J. A. *J. Chem. Phys.* **1980**, *72*, 4244.

(28) Pople, J. A.; Krishman, R.; Schlegel, H. B.; Binkley, J. S. *Int. J. Quantum Chem.* **1978**, *14*, 545.

(29) Raghavachari, K. *J. Chem. Phys.* **1985**, *82*, 4607.

(30) Pople, J. A.; Head-Gordon, M.; Raghavachari, K. *J. Chem. Phys.* **1987**, *87*, 5968.

(31) (a) Wales, D. J. *J. Chem. Soc., Faraday Trans.* **1990**, *86*, 3505. (b) McDowell, H. K.; Chiu, H.-L.; Geldard, J. F. *Inorg. Chem.* **1988**, *27*, 1674.

tioned in the Introduction, an alternative structure can be obtained when the auxiliary ligands are strong σ-donors with little or no π-donating capacity and are not too sterically bulky. The hydride ligand matches these criteria beautifully and, of course, is the least computationally demanding type. The molecules we initially selected for study, CrH_6 and WH_6,[32] are hypothetical ones. In fact, no d^0 MH_6 molecule has been reported, although d^6 FeH_6^{4-} and RuD_6^{4-} are known[33] along with several d^0 $MH_6(PR_3)_3$ examples.[34] We wish to present first a generalized description of the d^0 MH_6 situation before specific computational details are given.

The molecular orbital description for a d^0 MH_6 molecules at the octahedral geometry is shown on the left side of Figure 1. A small gap between the HOMO (t_{1u}) and LUMO (t_{2g}) implies a potential second-order Jahn–Teller driving force for distortions with normal modes of t_{2u} and t_{1u} symmetry. In CrH_6 at the optimized O_h geometry (vide infra), the frequencies for the t_{2u} and t_{1u} normal modes are computed to be imaginary at the MP2 level (2021i and 1891i cm^{-1}, respectively). A t_{2u} distortion involves rotation about one 3-fold axis to yield a trigonal prismatic D_{3h} structure. As indicated in Figure 1, two members of the empty t_{2g} set mix into and stabilize two components of the filled t_{1u} set. Since t_{2g} is metal d localized, the two stabilized molecular orbitals, now of e′ symmetry, become hybridized at the metal toward the hydrogens. Notice that one component of the t_{1u} set (a_2'') and one component of t_{2g} (a_1') are not affected by this distortion. It is then easy to see why many d^2 ML_6 complexes, where a_1' is filled, have structures along the $O_h \rightarrow D_{3h}$ path.[35] But for a d^0 molecule one should be able to achieve further stabilization by the pyramidalization mode of a_2'' symmetry, as shown on the right side of Figure 1. Empty a_1' then mixes into and stabilizes filled a_2''. For CrH_6 at the optimized D_{3h} geometry, there is, in fact, an imaginary a_2'' mode of 480i cm^{-1}. The $O_h \rightarrow D_{3h} \rightarrow C_{3v}$ path is only one of many distortions that should be stabilizing for a d^0 MH_6 complex. For example, pyramidalization about one of the 3-fold faces of the octahedron directly mixes all three components of t_{2g} into the t_{1u} set. A C_{2v} distortion couples one member of t_{2g} with t_{1u}.[12] In a local sense, the distortions in these situations (and many others) lead to increased d character for the metal–hydrogen bonds. This creates bonds which are more covalent, stronger, and shorter, as has been recognized in other contexts.[36] Figure 1 also demonstrates that the e_g set at the octahedral geometry is continuously destabilized on going from $O_h \rightarrow D_{3h} \rightarrow C_{3v}$. Overlap between the metal d and hydrogen s orbitals is decreased along the distortion path for these two molecular orbitals. Thus, the amount of stabilization afforded to the t_{1u} set is a critical factor. If the HOMO–LUMO gap is too large, then the distortion will not be energetically favorable. We will return to this point later. We also need to emphasize that the application of the Jahn–Teller method merely indicates a potential for distortion. It does not follow that the ground state for a molecule can be directly found by following one normal mode of distortion. The resulting stationary point may well be unstable with respect to further distortions.

Our initial optimizations of CrH_6 were at the HF level and led to a preponderance of η^2-H_2 and clustered-type structures. Previous work[37] has demonstrated that at the HF level η^2-H_2 structures are inordinately stabilized over metal dihydride isomers, in contrast to MP2 or other correlated techniques. What is more worrisome in this regard is that HF theory tends to give H–H distances that are systematically too short and M–H distances that are too long, and this deficiency is removed at the MP2 level. Therefore, all optimization was carried out using basis I at the MP2 level, and each stationary point was categorized by a frequency analysis at this level. The stationary points found are listed in Scheme I. The relative energies (kcal/mol) at the MP2 and MP4 levels for basis I and basis II, along with the number of imaginary frequencies for each structure, are listed in Table I. The arrows in Scheme I do not indicate, in general, specific reaction paths, which were not followed; rather, they illustrate sequential deformations. For convenience, an asterisk by a structure indicates the presence of one or more imaginary fre-

Scheme I

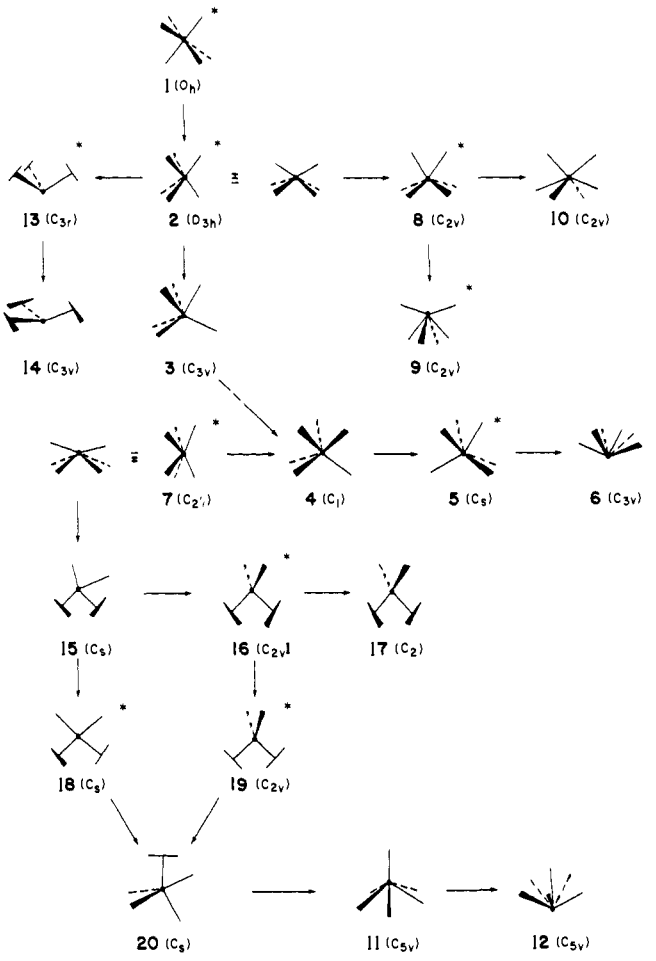

Table I. Relative Energies (kcal/mol) and Number of Imaginary Frequencies for CrH_6

	basis I		basis II	
structure	MP2	freq[a]	MP2	MP4
1, O_h	181	6	186	196
2, D_{3h}	46	3	53	39
3, C_{3v}	26	0	27	22
4, C_1	14	0	14	17
5, C_s	17	1	16	17
6, C_{3v}	0	0	0	3
7, C_{2v}	24	1	25	24
8, C_{2v}	30	2	33	39
9, C_{2v}	37	3		
10, C_{2v}	42	0		
11, C_{5v}	18	0	23	7
12, C_{5v}	3	0	4	0
13, C_{3v}	32	1	22	36
14, C_{3v}	16	0	5	24
15, C_s	17	0	12	24
16, C_{2v}	48	2		
17, C_2	45	0		
18, C_s	43	2		
19, C_{2v}	31	1	22	41
20, C_s	25	0	23	34

[a] The number of imaginary frequencies.

(32) Calculations of CrH_6 and WH_6 at the octahedral geometry have been reported: Pyykkö, P.; Desclaux, J. P. *Chem. Phys.* **1978**, *34*, 261.

(33) For computations, see: Lindberg, P.; Noreus, D.; Blomberg, M. R. A.; Siegbahn, P. E. M. *J. Chem. Phys.* **1986**, *85*, 4530.

(34) Hlatky, G. G.; Crabtree, R. H. *Coord. Chem. Rev.* **1985**, *65*, 1.

(35) (a) Kepert, D. L. *Prog. Inorg. Chem.* **1977**, *1*, 23. (b) Wentworth, R. A. D. *Coord. Chem. Rev.* **1972**, *9*, 171.

(36) (a) Dobbs, K. D.; Hehre, W. J. *J. Am. Chem. Soc.* **1986**, *108*, 4663. (b) Ohanessian, G.; Goddard, W. A., III *Acc. Chem. Res.* **1990**, *23*, 386.

(37) Chan, F.; Oishi, Y.; Albright, T. A., to be published.

quencies. Structures **1**, **2**, and **3** follow the deformation path presented in Figure 1. The stabilization energy on going from O_h (**1**) to D_{3h} (**2**) is immense—159 kcal/mol at the MP4 level using basis II—and that corresponding to the D_{3h} (**2**) to C_{3v} (**3**) sequence was found to be an additional 17 kcal/mol. Structures **5** and **6** can be viewed simply as resulting from pyramidalization about a 3-fold face of the octahedron or alternatively as a rotation of three hydrogens about the 3-fold axis from **3** to, ultimately, **6**. At the MP4 (basis II) level, **6** is stabilized by an additional 14 kcal/mol relative to **3**. In it, one set of three hydrogens makes an angle of 40.8°, while in the other set the angle is 77.8° with respect to the 3-fold axis. All six hydrogen atoms reside on one side of the chromium atom! The closest H···H contact between the two sets was still 1.61 Å, well outside any η^2-H_2 type structure. The corresponding H···H overlap population was computed (from the HF, basis I wave function) to be 0.058. While the overlap population is much smaller than that for an η^2-H_2 species (vide infra), it is still positive and not the sizable negative quantity expected for a typical nonbonded contact. Structures **7**–**10** represent C_{2v} distorted structures; all were found to lie very high in energy relative to **6**, for example. Two unique stationary points, **11** and **12**, were found when C_{5v} symmetries were considered.[38] **12** was computed to be at a lower energy. Here, the apical H–Cr–equatorial H angle is 64.3°. The H···H distances between the apical and equatorial hydrogens were 1.67 Å, with an overlap population of −0.011 (basis I). The H···H distances between adjacent equatorial hydrogens were 1.56 Å, with overlap populations of 0.032. Force field calculations interestingly predict that an ML_6 structure akin to **12** is the global minimum when a three-body potential with a sizable positive coefficient is included.[31a] In the geometries of **6**, **11**, and **12** especially, the hydrogens tend to cluster. There appear to be weak attractive forces between the hydrogens. Whether or not this feature remains when the structures are optimized with a more sophisticated electron correlation treatment will be the subject of future study. From work on the molecules in this study and elsewhere, we do know that HF optimized geometries produce structures that tend to have shorter H···H contacts.

For octahedral geometry **1** the optimal Cr–H distance was computed to be 1.69 Å. This diminishes to 1.58 Å in **2** and 1.52 and 1.55 Å in **3**. This nicely corresponds to the arguments given previously that as the distortion proceeds from **1** to **2** to **3** the Cr–H bonds develop more d character at chromium and this, in turn, makes them shorter and stronger. Even in the crowded structure of **6**, the Cr–H distances were found to be 1.58 and 1.57 Å, and in **12**, the equatorial distances were 1.56 Å while the axial one was 1.58 Å.

Structures **1**–**12** in Scheme I represent "classical" structures where, in a localized sense, one might think that there exist six two-center, two-electron bonds between chromium and hydrogen. Structures **13**–**20** contain one or more η^2-H_2 ligands coordinated to the metal. As mentioned previously, η^2-H_2 structures were found to be pervasive on the potential energy surface of CrH_6. Optimizations of all trigonal bipyramidal-based $(\eta^2\text{-}H_2)CrH_4$ structures produced only one stationary point, **20**, where the η^2-H_2 structure remained intact. Bis(η^2-H_2) tetrahedral stationary points are given by **15**–**19**. Notice that these are all at high relative energies from Table I. For reference purposes, and these are typical values, the H–H distances in **20** and **17** were 0.83 and 0.80 Å, respectively. The corresponding H–H overlap populations (basis I) were 0.489 (**20**) and 0.508 (**17**). Two tris(η^2-H_2) structures were found, **13** and **14**; both have C_{3v} symmetry. **14** was computed to be 12 kcal/mol more stable than **13** at the MP4 level using basis II. Structure **13** had one imaginary frequency of a_2 symmetry, corresponding to rotation about each Cr–H_2 axis to yield **14**. The structure of **14** deserves special comment. The H–H distance for the η^2-hydrogens was 1.04 Å. This is considerably longer than that for any other η^2-H_2 structure. The H–H overlap population of 0.164 (basis I) is also much smaller than for any of the other η^2 complexes. It is clear that back-donation to H_2 σ^* is very strong in this structure. The H···H distance between H_2 units was found to be 1.77 Å. What is surprising is the computed H···H overlap population of 0.066 (basis I). This value is larger than that found for any other "nonbonded" pair. The implication is that there is some interaction between the H_2 units. This is not an artifact of the basis set on hydrogen. Three H_2 units (with an optimal H–H distance of 0.738 Å) were placed in a D_{3h} arrangement. Fixing the nonbonded H···H distance to be 1.77 Å required 11.4 kcal/mol using basis II at the MP4 level.[39] This situation can also be viewed as originating from some, although certainly incomplete, delocation in the H_6 unit as a whole. We shall explore this topic fully for $(\eta^2\text{-}H_2)_3Cr$ and other molecules elsewhere.

Certainly there are other stationary points on the potential energy surface of CrH_6. For example, there is probably a transition state with C_{5v} symmetry that links structure **11** by pyramidalization to **12**. From the relative energies in Table I, it would appear that either structure **6** or **12** represents the ground-state minimum. Notice that structure **14** at the MP2 level with basis set II is also at a low relative energy. These three structures, along with **1**, **3**, and **4**, were selected for further study by augmentation of f functions to Cr in basis II (yielding basis III) and the utilization of other correlation treatments. The results are listed in Table II along with the HF relative energies. Recall that all structures have been optimized at the MP2 level with basis I and that all structures are computed to be minima on the potential energy surface with the exception of the octahedral structure (**1**). Our thought was that the addition of f functions might stabilize clustered structures like **6**, **12**, and **14**. Inspection of Table II shows that the relative energies on going from basis II and basis III do not change appreciably. In fact, there is generally not much difference between basis I and basis II, although there are a few exceptions (e.g., structures **13** and **19** at the MP2 level in Table I along with **14** at the MP2 and QCISD levels in Table II). Unfortunately, this is not the case when the correlation treatments are compared.

To begin the discussion, notice from Table II that at the HF level the relative energy of O_h CrH_6 is still extraordinarily high. However, the energy of $(\eta^2\text{-}H_2)_3Cr$, **14**, and *all* η^2-H_2 species are put at much too low a relative energy. In other words, and we have found this to be true for other molecules,[37] HF theory greatly underestimates the stability of two metal–hydride bonds relative to a metal–(η^2-H_2) three-center, two-electron bond and a localized lone pair in a d orbital at the metal. On the other hand, MP2

Table II. Relative Energies (kcal/mol) for Several CrH_6 Structures

		structure					
method	basis	**1** (O_h)	**3** (C_{3v})	**4** (C_1)	**6** (C_{3v})	**12** (C_{5v})	**14** (C_{3v})
HF	I	138	38	57	45	60	0
	II	143	43	65	53	68	0
	III	140	42	64	53	68	0
MP2	I	181	26	14	0	3	15
	II	186	27	14	0	4	5
	III	191	28	32	0	3	5
MP4	II	196	22	17	3	0	24
	III	202	22	32	4	0	26
CCD	I	143	20	29	9	19	0
	II	153	25	36	17	27	0
	III	157	27	38	18	28	0
ST4CCD	I	144	7	19	2	9	0
	II	158	14	26	10	16	0
	III	162	15	27	10	17	0
QCISD	I	163	0	22	4	7	13
	II	166	0	21	4	8	2
	III	171	0	22	5	8	4
QCISD(T)	I	146	0	19	0	9	2
	II	161	8	26	8	17	0
	III	165	10	32	10	20	0

(38) C_{6v} and D_{6h} structures using basis I were found to lie at much higher energies and are not reported here.

(39) This does not include basis set superposition error which should be small with the 6-311G** basis.

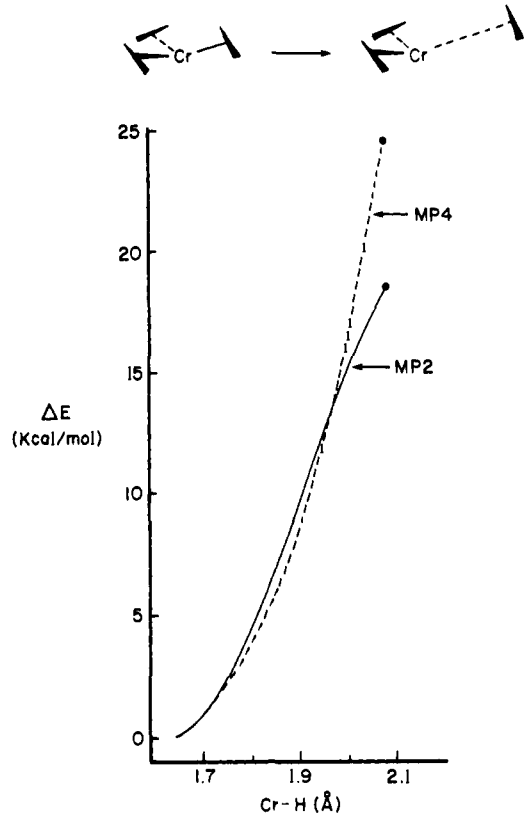

Figure 2. Potential energy curves for dissociation of one H_2 unit from $(\eta^2\text{-}H_2)_3Cr$, **14**.

calculations do overestimate the stability of "classical" metal hydrides, on the basis of comparisons to experimentally determined relative energies,[37] and we suspect that this is also the case here. Unfortunately, going to the MP4 level simply accentuates this tendency. Notice from Table I that the relative energies of **13**, **14**, **15**, **19**, and **20** consistently increase upon going from the MP2 to MP4 treatments. The CCD and ST4CCD treatments unambiguously point to the $(\eta^2\text{-}H_2)_3Cr$ structure (**14**) as being the most stable. At the QCISD level, **3**, **6**, and **14** appear to be viable contenders for the ground-state minimum, with **12** not too far away. Inclusion of triple substitutions in the QCISD framework again points to **14** as the ground-state minimum. This does not appear to be a multireference problem. Two sets of pilot calculations were carried out on **1** and **6**. CASSCF calculations with basis I were carried out using the three highest occupied orbitals and three virtual levels (in **6** they are of a_1 + e symmetry; in **1**, of e_g and a_{1g} symmetry). The energy of **6** was found to be 140 kcal/mol lower than that of **1**. Importantly, the HF determinant had coefficients of 0.92 and 0.93 for **1** and **6**, respectively. The problem here is that, at least in **1**, the active virtual space must be very carefully chosen. For example, using the three lowest virtual levels of t_{2g} symmetry produces a solution for **1** which is 16 kcal/mol higher in energy. Thus, for a general treatment which puts structures like **6**, **12**, and **14** on equal footing, a CASSCF approach necessitates the utilization of all six filled orbitals (with 12 electrons) and a large virtual active space. This is computationally very demanding. Using the six filled and the lowest 12 virtual orbitals as the active space, a MCSCF wavefunction for **1** and **6** was constructed for all single and double substitutions. The HF determinants had a coefficient of 0.93 for **1** and **6**, with **6** lying 134 kcal/mol lower in energy. What is clear from Table II is that the C_1 structure **4** is not likely to be the lowest-energy minimum and that the VSEPR mandated octahedral structure is, in fact, by far the highest-energy structure. In conclusion, it would appear that $(\eta^2\text{-}H_2)_3Cr$ (**14**) is the lowest-energy species from our calculations. The two other C_{3v} structures, **3** and **6**, may, in fact, be viable contenders at higher computational levels. In the introduction to this section we discussed how the three

Scheme II

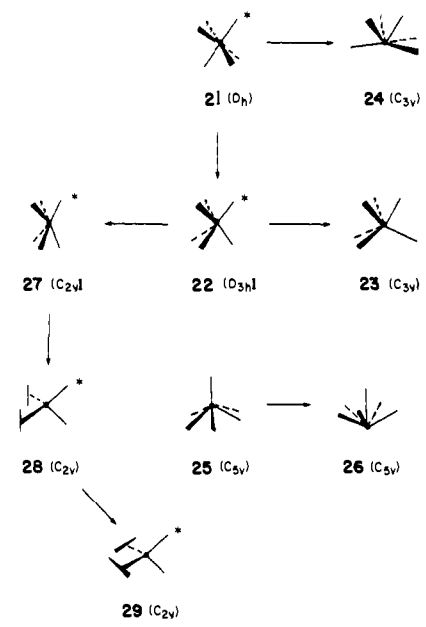

Table III. Relative Energies (kcal/mol) and Number of Imaginary Frequencies for WH_6

structure	HF	MP2	freq[a]	MP4(SDQ)	QCISD	QCISD(T)
21, O_h	126	145	6	140	142	142
22, D_{3h}	25	29	3	26	26	26
23, C_{3v}	0	0	0	0	0	0
24, C_{3v}	11	6	0	8	8	8
25, C_{5v}	2	2	0	1	1	1
26, C_{5v}	22	14	0	16	16	16
27, C_{2v}	24	25	1	25	25	25
28, C_{2v}	35	63	2	61	59	60
29, C_{2v}	25	48	2	46	46	46

[a] The number of imaginary frequencies.

members of empty t_{2g} at the octahedral geometry mix in and stabilize the filled t_{1u} set upon distortion to structures **3** and **6**. Notice that the geometrical motion required for going from **6** to **14** is rather slight; maximal use of d orbitals for bonding in **14** is retained.

The low energy of $(\eta^2\text{-}H_2)_3Cr$ (**14**) worried us in that it might lead to dissociation of one or more H_2 units. The electronic state for CrH_4 has been found to be $^3A_2$ by other workers,[40a] and, thus, dissociation of one H_2 unit would be spin-forbidden. Nonetheless, we carried out a test where one H_2 unit was stretched from **14** by sequential degrees and the structure was reoptimized in C_s symmetry at the MP2 level using basis I. Each point was then recomputed with basis II at the MP2 and MP4 levels. The potential energy curves thus generated are displayed in Figure 2. For the final point computed in Figure 2, the H–H distance for the H_2 unit undergoing dissociation contracted to 0.80 Å while the remaining H_2 units elongated slightly (from 1.03 Å in **14**) to 1.06 Å. It is clear that at this level of theory, $(\eta^2\text{-}H_2)_3Cr$ represents a bound molecule.

The potential energy surface for WH_6 was investigated via HF and MP2 optimizations. The stationary points found are illustrated in Scheme II, where an asterisk by a structure denotes a transition state or higher-order saddle point. The corresponding relative energies, along with the number of imaginary frequencies (at the MP2 level), are reported in Table III. The differences between HF and MP2 techniques both in terms of geometrical parameters and relative energies are quite modest, except for the two bis-$(\eta^2\text{-}H_2)$ species, **28** and **29**, where the trends are identical to those presented previously for CrH_6.

(40) (a) Hood, D. M.; Pitzer, R. M.; Schaeffer, H. F., III *J. Chem. Phys.* **1979**, *71*, 705. (b) Shen, M.; Schaeffer, H. F., III; Partridge, H. *J. Chem. Phys.* **1993**, *98*, 508.

The energy stabilization predicted via the one-electron arguments in Figure 1 for the O_h (**21**) → D_{3h} (**22**) → C_{3v} (**23**) distortion path is again nicely confirmed. The O_h isomer was found to be 142 kcal/mol higher in energy than the C_{3v}, **23**, at the QCISD(T) level. The calculations at all levels of theory predict **23** to be the global minimum. As a result of the increased d orbital mixing in **23**, the MP2 bond distances, on going from **21** to **23**, decrease from 1.83 to 1.69 and 1.73 Å. Direct pyramidalization of **21** also yields another C_{3v} minimum, **24**, which is slightly higher in energy than **23**. There is somewhat less distortion in **24** compared to its CrH_6 analog **6**. Here, one set of three hydrogens makes an angle of 37.2° with respect to the 3-fold rotation axis while the other set makes an angle of 93.9° at the MP2 level. Two C_{5v} structures, **25** and **26**, were also found with **25** lying only 1 kcal/mol above **23**. Very recently Shen, Schaefer, and Partridge[40b] have carried out all-electron ab initio calculations of WH_6 at the MP2, CCSD, and modified coupled pair functional (MCPF) levels. Their optimized structures for **21**–**25** and the relative energies are in very close agreement with our values. Three additional stationary points were found on the potential energy surface; however, their relative energies are much higher than those associated with **23**–**26**. At the MCPF level with relativistic effects estimated using the Cowan–Griffin corrections (which are also employed in our effective core potentials), the authors in fact find that **25** is 0.4 kcal/mol more stable than **23**.[40b] We shall return to this point later. Only two η^2-H_2 structures, **28** and **29**, were found on the potential energy surface. Furthermore, both lie at high energies relative to **23**. All of the stationary points found for CrH_6 were also investigated for WH_6. Specifically, $(\eta^2\text{-}H_2)_3W$ structures, analogs of **13** and **14** (Scheme I), collapsed upon optimization to **23** and **24**, respectively. The lack of η^2-H_2 structures, prevalent for CrH_6, can be viewed as a consequence of the observation[41] that higher oxidation states are much more stable for the heavier transition-metal elements than for those of the first transition-metal series.[42] Alternatively, it is well-known that the more diffuse 5d orbital, as opposed to a 3d orbital, overlaps to a greater extent with the hydrogen 1s orbital. For example, Ohanessian and Goddard[36b] have found that the percentage of d character in the M–H bond rises from 45% in CrH^+ to 60% in WH^+. Thus, back-donation from a filled metal d orbital to H_2 σ^* is expected to be larger for W compared with Cr. As a consequence, an $(\eta^2\text{-}H_2)M$ species will have an increased propensity to rearrange to a classical MH_2 structure as one descends a column in the periodic table.[43] In conclusion, either C_{3v} **23** or C_{5v} **25** is the global minimum; at all computational levels the energy difference between them is very small in both our and Shen, Shaefer, and Partridge's work.[40b] The Jahn–Teller arguments for the stability of **23** have been presented previously. For **25** (or **26**) we note that symmetry-adapted linear combinations for the hydrogen s orbitals span the $a_1 + e_1 + e_2$ irreducible representations which are just those given by the metal d orbitals. Thus, d orbital bonding to the hydrides is beautifully maximized in structure **25**.

Charging effects at the metal are very important in setting the energy differences. We have previously shown[14] that at the HF level the O_h structure for TiH_6^{2-} is more stable than D_{3h}.[44-46] At the MP2 and MP4 levels, this ordering is reversed with D_{3h} being 3.2 and 9.2 kcal/mol, respectively, more stable using basis II. Distortions toward C_{3v}, C_{2v}, etc., symmetry were explored in each structure. No additional stationary points were located. Certainly, Ti is more electropositive than Cr or W and the bonding in TiH_6^{2-} is much more ionic than that for CrH_6 and WH_6. Thus, in a one-electron sense the t_{2g} set (Figure 1) for TiH_6^{2-} at the octahedral geometry is expected to lie higher in energy in comparison to CrH_6 and WH_6, and the energy potential associated with a second-order Jahn–Teller distortion is greatly diminished. In agreement with this are the recent ab initio results of Chakin and co-workers,[44] who found that the O_h/D_{3h} energy differences at the HF level lie in the order: $ScH_6^{3-} < TiH_6^{2-} < VH_6^- < CrH_6 < MnH_6^+$, where the O_h isomer was found to be the more stable one for ScH_6^{3-} and TiH_6^{2-}. Thus, there is considerable latitude in the deformation potentials and available structures for the d^0 MH_6 system. We now turn our attention to molecules that are experimentally known.

Scheme III

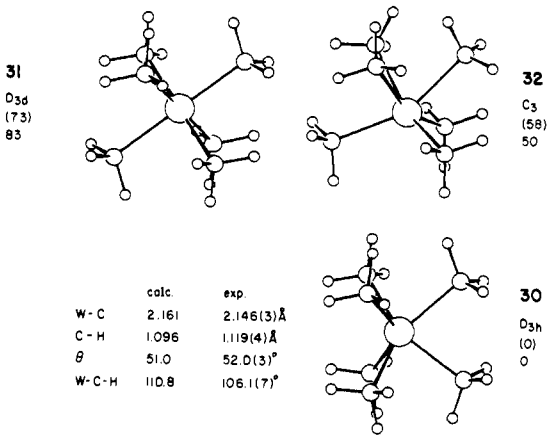

WMe_6 and MF_6

Shortland and Wilkinson reported the preparation of WMe_6 in 1973.[47] Until very recently its structure was assumed to be octahedral. The strong covalent bonding between tungsten and the methyl groups, using the arguments centered around Figure 1, should cause the octahedron to be less stable than a distorted variant where greater d orbital involvement in the bonding exists. In fact, Haaland and co-workers' electron diffraction results[48] pointed to a trigonal prismatic or slightly distorted C_{3v} structure. The experimental radial distribution curve was inconsistent with an octahedral geometry. Likewise, Morse and Girolami[49] have reported the X-ray crystal structure of $[Li(TMEDA)]_2[ZrMe_6]$. The $ZrMe_6^{2-}$ framework was found to be trigonal prismatic. On the basis of the similarity between HF and MP2 optimized geometries for WH_6, all geometry optimizations were carried out for WMe_6 at the HF level with single-point MP2 calculations. The results are shown in Scheme III. The molecular symmetry imposed, along with relative energies in kcal/mol (those listed in parentheses are the HF values), is reported alongside each structure. We find trigonal prismatic **30** to be the global minimum. As indicated in the scheme, our HF optimized geometry[50] is in excellent agreement with the electron diffraction data.[48] The octahedral isomer **31** was computed to be 83 kcal/mol higher in energy than **30**. Direct pyramidalization of the octahedron yielded a C_{3v}-type structure (**32**); however, this is also computed to lie at a very high energy. We looked very carefully for potential distortions of **30** toward a C_{3v} variant analogous to **23** for WH_6. Several attempts at minor distortions resulted in the collapse back

(41) (a) Cotton, F. A.; Wilkinson, G. *Advanced Inorganic Chemistry*, 5th ed.; John Wiley: New York, 1988; 777. (b) Huheey, J. E. *Inorganic Chemistry*, 3rd ed.; Harper and Row: New York, 1983; 578.

(42) The calculated adiabatic electron affinity of WF_6 was found to be 3.85 eV, while that in CrF_6 was 8.24 eV. Miyoshi, E.; Sakai, Y.; Murakami, A.; Iwaki, H.; Terashima, H.; Shoda, T.; Kawqaguchi, T. *J. Chem. Phys.* **1988**, *89*, 4193.

(43) For experimental support, see: Bautista, M. T.; Cappellani, E. P.; Drouin, S. D.; Morris, R. H.; Schweitzer, C. T.; Sella, A.; Zubkowski, J. *J. Am. Chem. Soc.* **1991**, *113*, 4876 and references therein.

(44) (a) Musaev, D. G.; Charkin, O. P. *Koordinat. Khim.* **1989**, *15*, 161. (b) Zjubin, A. S.; Musaev, D. G.; Charkin, O. P. *Russ. J. Inorg. Chem.* In press.

(45) Cameron, A. D.; Fitzgerald, G.; Zerner, M. C. *Inorg. Chem.* **1988**, *27*, 3437.

(46) (a) Jonas, V.; Frenking, G.; Gauss, J. *Chem. Phys. Lett.* **1992**, *194*, 109. (b) These researchers found that TiH_6^{2-} is 3.7 and 2.9 kcal/mol more stable at the D_{3h} geometry at the QCISD(T) and CCSD(T) levels, respectively. (c) In a reference to unpublished work the O_h geometry for CrF_6 was found to be 11.2 kcal/mol more stable at the CCSD(T) level.

(47) Shortland, A. J.; Wilkinson, G. *J. Chem. Soc., Dalton Trans.* **1973**, 872. Galyer, A. L.; Wilkinson, G. *Ibid.* **1976**, 2235.

(48) Haaland, A.; Hammel, A.; Rypdal, K.; Volden, H. V. *J. Am. Chem. Soc.* **1990**, *112*, 4547.

(49) Morse, P. M.; Girolami, G. S. *J. Am. Chem. Soc.* **1989**, *111*, 4114.

(50) There are two types of C–H bonds in **30** in the ratio of 1:2. The C–H distance and W–C–H angles are averaged from those found to be 1.093 and 1.097 Å along with 111.5° and 110.4°, respectively.

to the D_{3h} structure **30**. Ultimately, the angular deformation provided by **23** for WH_6 was used, and an optimal orientation of each methyl group at this structure was located. The optimization was then carried out in C_1 symmetry,[51] and this also collapsed back to **30**. Thus, we are reasonably certain that **30** represents the global minimum. The He(I) and He(II) photoelectron spectra[52] of WMe_6 should then be reassigned, according to our HF calculations, as ionizations from the a_2'', e', and e'' W–C σ-bonding orbitals (in order of increasing ionization potential). The a_1' orbital lies at the top edge of the C–H σ-bonding manifold. In view of the similarity between the photoelectron spectra of WMe_6 and d^1 $ReMe_6$,[52] we suspect that $ReMe_6$ is also trigonal prismatic, contrary to previous speculations,[52,53] with the extra electron in a metal-centered d orbital of a_1' symmetry (see Figure 1).

According to the model presented in the Introduction, when the ligands are electronegative the t_{1u} set (see Figure 1) lies at a lower energy relative to t_{2g}. Alternatively, if the ligands possess strong π-donating capability, then they will interact with and destabilize t_{2g}. Either (or both) perturbation increases the t_{1u}–t_{2g} energy gap, and, thus, the second-order stabilization energy associated with one or more members of the t_{1u} set will be greatly diminished. The VSEPR-mandated octahedral geometry can be rendered more stable than the trigonal prismatic or other structural variants. WF_6 nicely illustrates this, where the geometry in the gas phase[54] and in the solid state[55] has been found to be O_h. At the HF level, we find the W–F bond distance to be 1.835 Å, which is in very good agreement with the electron diffraction values of 1.833(8)[54a] and 1.832(3) Å.[54b] The O_h isomer was found to be 14 kcal/mol more stable than the optimized D_{3h} one, and this increases to 16 kcal/mol by single-point MP2 calculations. The structures of MoF_6,[54b,56] WBr_6,[57] WCl_6,[58] TiF_6^{2-} (with three different countercations),[59] $ZrCl_6^{2-}$,[60] and $ZrCl_4F_2^{2-}$[60b] have all been found to be octahedral. Amido or alkoxide ligands are strong π-donors; consequently, $W(NMe_2)_6$,[61] $Mo(NMe_2)_6$,[62] and $W(OMe)_6$[63] have been shown to possess an octahedral geometry. A controversy has arisen over the geometry and existence of CrF_6, first reported in 1963.[64] The original matrix isolation work by Hope et al.[65] postulated that CrF_6 was octahedral on the basis of its IR spectrum. This was challenged by Jacob and Willmer,[66] who argued that the material was CrF_5. Our initial theoretical calculations[14] using basis I at the MP2 level put the O_h isomer

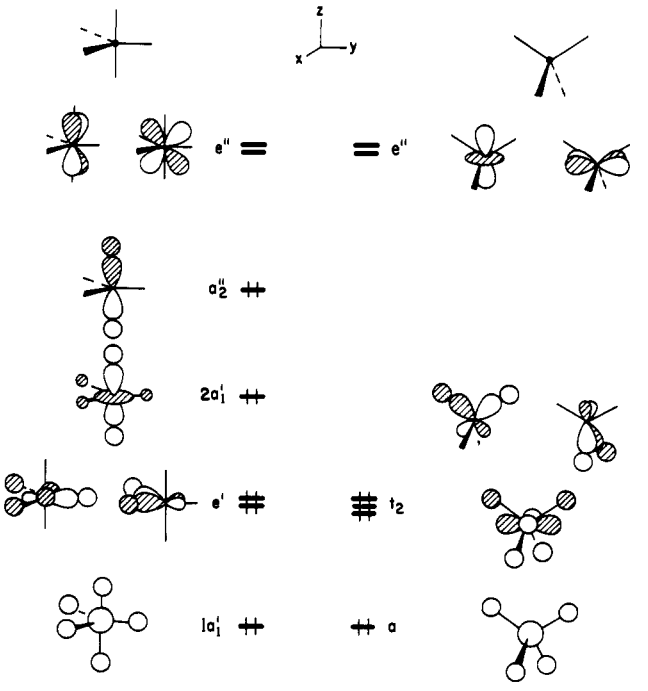

Figure 3. Valence orbitals of a d^0 MH_5 (left) and d^0 MH_4 (right) molecule. Note that the metal p_z hybridization for the x^2-y^2 component of t_2 has not been included in the drawing.

Scheme IV

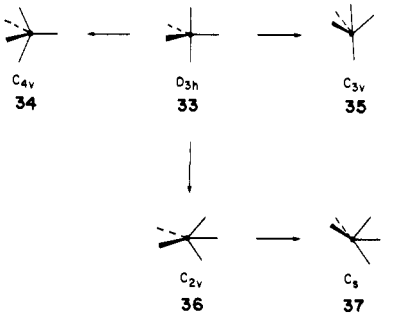

of CrF_6 18.5 kcal/mol more stable than D_{3h}. This decreases to 12.2 kcal/mol when using basis II (MP2). Marsden and Wolynec[67] found using CCD calculations that the D_{3h} structure was 4.7 kcal/mol more stable and further that the MPn expansion was oscillatory.[68] Using our basis I, we have reconfirmed this result in that the D_{3h} geometry is 7.3 kcal/mol more stable than O_h at the CCD level. However, we find that with the ST4CCD treatment this ordering is reversed and the D_{3h} structure now lies 22.6 kcal/mol higher in energy.[46c] The resolution of this controversy comes from the recently published communication of Hope and co-workers.[69] The high-resolution IR spectrum shows isotopic features which can be modeled only for CrF_6 (and not for CrF_5); furthermore, it is convincingly demonstrated that CrF_6 is, indeed, octahedral.[69]

d^0 ML_5 Complexes

For a d^0 ML_5 complex the VSEPR rules and force field calculations[31b] predict that a trigonal bipyramidal structure should be more stable than other geometrical alternatives. A number of theoretical studies have been previously carried out for structural

(51) The only constrainis imposed were that all C–H bond lengths were equivalent and that the WC_6 core retained C_{3v} symmetry. This leads to 49 independent variables which required 6.5 days of CPU time on a VAX 8650.

(52) Green, J. C.; Lloyd, D. R.; Galyer, L.; Mertis, K.; Wilkinson, G. *J. Chem. Soc., Dalton Trans.* **1978**, 1403.

(53) Gibson, J. F.; Lack, G. M.; Mertis, K.; Wilkinson, G. *J. Chem. Soc., Dalton Trans.* **1976**, 1492.

(54) (a) Kimura, M.; Schomaker, U.; Smith, D. W.; Weinstock, B. *J. Chem. Phys.* **1968**, *48*, 4001. (b) Seip, H. M.; Seip, R. *Acta Chem. Scand.* **1966**, *20*, 2698.

(55) Levy, J. H.; Taylor, J. C.; Wilson, P. W. *J. Solid State Chem.* **1975**, *15*, 360.

(56) Levy, J. H.; Taylor, J. C.; Wilson, P. W. *Acta Crystallogr., Sect. B* **1975**, *31*, 398. Levy, J. H.; Sanger, P. L.; Taylor, J. C.; Wilson, P. W. *Ibid.* **1975**, *31*, 1065.

(57) Willing, W.; Müller, U. *Acta Crystallogr., Sect. C* **1987**, *43*, 1425.

(58) Taylor, J. C.; Wilson, P. S. *Acta Crystallogr., Sect. B* **1974**, *30*, 1216.

(59) Kojić-Prodić, B.; Matković, B.; Ščavnicar, S. *Acta Crystallogr., Sect. B* **1971**, *27*, 635. Golič, L.; Kaučič, V.; Kojić-Prodić, B. *Ibid.* **1980**, *36*, 659. Schäfer, G. F. *Z. Kristallogr.* **1986**, *175*, 269.

(60) (a) Schmidbaur, H.; Pichl, R.; Müller, G. *Z. Naturforsch.* **1986**, *41b*, 395. (b) Hartmann, E.; Dehnicke, K.; Fenske, D.; Goesmann, H.; Baum, G. *Ibid.* **1989**, *44b*, 1155.

(61) (a) Galyer, A.; Wilkinson, G. *J. Chem. Soc., Dalton Trans.* **1976**, 2235. (b) Hagen, K.; Holwill, C. J.; Rice, D. A.; Runnacles, J. D. *Acta Chem. Scand.* **1988**, *A42*, 578.

(62) Chisholm, M. H.; Hammond, C. E.; Huffman, J. C. *J. Chem. Soc., Chem. Commun.* **1987**, 1423.

(63) Haaland, A.; Rypdal, K.; Volden, H. V.; Jacob, E.; Weidlein, J. *Acta Chem. Scand.* **1989**, *43*, 911.

(64) Glemser, O.; Roesky, H.; Hellberg, K. H. *Angew. Chem., Int. Ed. Engl.* **1963**, *2*, 266.

(65) Hope, E. G.; Jones, P. J.; Leavason, W.; Ogden, J. S.; Tajik, M.; Turff, J. W. *J. Chem. Soc., Dalton Trans.* **1985**, 1443.

(66) Jacob, E.; Willner, H. *Chem. Ber.* **1990**, *123*, 1319.

(67) Marsden, C. J.; Wolynec, P. P. *Inorg. Chem.* **1991**, *30*, 1682.

(68) We concur that this is indeed the case. Frenking and co-workers[46a] also find similar tendencies for TiH_6^{2-} and VH_6^-. The results reported in Tables I and II for CrH_6 do indicate a problem with especially the relative energies of η^2-H_2 structures in a MPn expansion, as indicated previously. However, there is close correspondence in general between the HF and MP2 relative energies as well as those found at higher correlation levels for the remaining molecules investigated in this study.

(69) Hope, E. G.; Levason, W.; Ogden, J. S. *Inorg. Chem.* **1991**, *30*, 4873.

Table IV. Relative Energies for d^0 ML_5 Complexes

molecule	level	D_{3h} (33)	C_{4v} (34)	C_{3v} (35)	C_{2v} (36)	C_s (37)
VF_5 basis I	HF	0(0)[a]	1.6(1)[a]	[b]	[b]	[b]
	MP2	0	0.7			
VF_5 basis II	HF	0	2.0			
	MP2	0	0.8			
$TaCl_5$	HF	0(0)	1.7(1)			
	MP2	0	1.6			
	MP4(SDQ)	0	1.5			
	QCISD	0	1.7			
	QCISD(T)	0	1.7			
TaH_5	HF	16.6	0	16.6	3.0	
	MP2	20.2(3)	0(0)	20.1(2)	3.4(1)	
	MP4(SDQ)	19.1	0	19.1	3.3	
	QCISD	19.3	0	19.3	3.2	
	QCISD(T)	19.6	0	19.6	3.1	
VH_5 basis I	HF	20.9	0	16.4	0.5	4.7
	MP2	27.5(3)	0(0)	21.5(2)	6.5(2)	4.9(1)
	MP4(SDQ)	27.9	0	23.3	5.8	6.2
	QCISD	29.4	0	24.9	3.0	5.0
	QCISD(T)	27.4	0	22.6	3.2	5.4

[a] The number of imaginary frequencies are given in parentheses. [b] Statioinary points are not found on the potential energy surface.

preferences of transition-metal complexes with greater than d^0 electron counts.[8,70] The valence orbitals for a D_{3h} structure are shown on the left side of Figure 3. Notice the presence of the high-lying, filled a_2'' orbital which consists of p character at the metal and the low-lying e'' set which is exclusively metal d. It is clear that these orbitals can play a role precisely analogous to the t_{1u}/t_{2g} set (Figure 1) for ML_6. A potential second-order Jahn–Teller distortion of $e'' \times a_2'' = e'$ symmetry will serve to mix e'' into a_2'', stabilizing the latter. Provided that the e''–a_2'' energy gap is small, this e' distortion mode, which can convert the trigonal bipyramid to the square pyramid (C_{4v}), will be stabilizing. As for the d^0 ML_6 example, this will occur when L contains little π-donating capabilities and the M–L bond is reasonably covalent. The D_{3h} and C_{4v} structures are, however, two of several possibilities to consider, as outlined in Scheme IV. We start our discussion with VF_5 and $TaCl_5$ where the potential energy surfaces are quite simple and there is ample experimental information.

The electron diffraction structure[71] of VF_5 points to a D_{3h} structure with axial and equatorial distances of 1.732(7) and 1.704(5) Å, respectively. Our HF calculations with basis I are in excellent agreement with optimized distances of 1.734 and 1.696 Å, respectively. Calculations of the harmonic frequencies produce values which are uniformly larger than the experimental gas-phase values[72] with a mean 7.2% error.[73] The symmetry of the normal modes associated with these frequencies agrees with the experimental assignments.[74] It has been universally argued[70a,b] that axial–equatorial exchange in VF_5 and other d^0 MX_5 molecules occurs via the classic Berry pseudorotation process[74] which proceeds from the D_{3h} (33) to C_{4v} (34) transition state in Scheme IV. Analysis of the ν_7 (e') vibrational transitions in VF_5 put the barrier height at 1.5–1.2 kcal/mol.[72c] Our calculations at the HF and MP2 (single-point) levels are reported in Table IV and are in agreement with this estimate.[75] By the Berry process, the one calculated imaginary mode of b_2 symmetry for the C_{4v} isomer does, indeed, take C_{4v} to D_{3h}. The situation for $TaCl_5$ is not quite so clear. The electron diffraction structure of $TaCl_5$ by Ischenko and co-workers was found to be D_{3h} with axial and equatorial bond lengths of 2.369(4) and 2.227(4) Å, respectively. Our axial distance was computed at the HF level to be 2.369 Å; however, the equatorial one was 2.326 Å. An error of this magnitude for theory is certainly not without precedent in the transition-metal area. However, there are a number of perplexing features of the experimental work in comparison to what has been found for other MX_5 molecules. Firstly, the gas-phase electron diffraction structures for NbF_5,[77] TaF_5,[77] and $TaBr_5$[76] (all have D_{3h} symmetry), along with the previously mentioned VF_5,[71] have axial–equatorial bond length differences of 0.07, 0.04, 0.06, and 0.03 Å, respectively. These are considerably smaller than that found[76] for $TaCl_5$ (0.14 Å). Ischenko and co-workers[76] also determined the axial and equatorial bond lengths for $NbCl_5$ to be 2.338(6) and 2.241(4) Å, respectively (a 0.10-Å difference). Optimizations[79] of $NbCl_5$ with five different basis sets (both all-electron and effective core potential) produce axial bond lengths that range from 2.356 to 2.373 Å. However, again the equatorial ones are predicted to be considerably shorter than those given by electron diffraction, 2.305–2.338 Å (axial–equatorial differences of 0.02–0.05 Å). The force fields used by Ischenko and co-workers[76] for the electron diffraction determination was developed from frequencies recorded and assigned by Beattie and Ozin.[80] There is a 5.7% absolute mean error between our calculated (harmonic) and the experimental values; however, there is a disagreement in the assignments. The peak at 181 cm^{-1} (calculated 192 cm^{-1}) was assigned to be of e' symmetry, but we find it to be an e'' mode. Likewise, that at 127 cm^{-1} (calculated 140 cm^{-1}) was assigned to be e'', whereas we find it to be e'. Furthermore, the low-frequency e' mode at 54 cm^{-1} (calculated 56 cm^{-1}) corresponds to the in-plane equatorial bend and that at 181 cm^{-1} to the axial–equatorial bending mode from the force field developed and used by Ischenko and co-workers.[76] Our calculations suggest that the 54 cm^{-1} vibration should correspond to the axial–equatorial bending motion and that at 127 cm^{-1} to the in-plane equatorial mode. We should point out that the relative ordering of the magnitudes, symmetries, and associated eigenvectors for the two sets of e' and e'' vibrations calculated for $TaCl_5$ correspond to those found from experiment and theory for VF_5. Thus, we encourage a reinvestigation of $TaCl_5$. Our calculations barrier heights on going from D_{3h} to C_{4v} at several correlated levels for $TaCl_5$ are presented in Table IV. Values from 1.5 to 1.7 kcal/mol are found, and this is in reasonable agreement with the estimate of 1.2(6) kcal/mol by Ischenko and co-workers.[76] At the C_{4v} geometry, one normal mode of b_2 symmetry was found to be imaginary, confirming that this structure was the transition state for the Berry pseudorotation process. For both VF_5 and $TaCl_5$, stationary points for D_{3h} and C_{4v} were the only ones located on the potential energy surface.

A d^0 MH_5 molecule is unknown, although the d^8 complexes Mg_2CoH_5 and Sr_2IrD_5 have been prepared and possess trigonal bipyramidal structures.[81] For a d^0 MH_5 molecule, the e''–a_2'' (Figure 3) energy gap is expected to be much smaller than that for MX_5. Consequently, non-VSEPR geometries are more likely to be present. We find this to be, indeed, the case. For TaH_5,

(70) (a) A review of the early literature may be found in Boldrev, A. I.; Charkin, O. P. *Zh. Strukt. Khim.* **1984**, *25*, 102. (b) Rossi, A. R.; Hoffmann, R. *Inorg. Chem.* **1975**, *14*, 365. (c) Elian, M.; Hoffmann, R. *Ibid.* **1975**, *14*, 1058. (d) Burdett, J. K. *Ibid.* **1975**, *14*, 375; *J. Chem. Soc., Faraday Trans. 2* **1974**, 1599. (e) Demuynck, J.; Strich, A.; Veillard, A. *Nouv. J. Chim.* **1977**, *1*, 217. (f) Hay, P. J. *J. Am. Chem. Soc.* **1978**, *100*, 2411. (g) Jean, Y.; Eisenstein, O. *Polyhedron* **1988**, *7*, 405. Rachidi, El-I. I.; Eisenstein, O.; Jean, Y. *New J. Chem.* **1990**, *14*, 671. Riehl, J.-F.; Jean, Y.; Eisenstein, O.; Pelissier, M. *Organometallics* **1992**, *11*, 729.

(71) Hagen, K.; Gilbert, M. M.; Hedberg, L.; Hedberg, K. *Inorg. Chem.* **1982**, *21*, 2690 and references therein.

(72) (a) Claassen, H. H.; Selig, H. *J. Chem. Phys.* **1966**, *44*, 4039. (b) Hope, E. G. *J. Chem. Soc., Dalton Trans.* **1990**, 723. (c) Bernstein, L. S.; Abramowitz, S.; Levin, I. W. *J. Chem. Phys.* **1976**, *64*, 3228. (d) Selig, H.; Holloway, J. H.; Tyson, J.; Claassen, H. H. *Ibid.* **1970**, *53*, 2559.

(73) The errors range from 3.7% to 9.9%.

(74) Berry, R. S. *J. Chem. Phys.* **1960**, *32*, 933.

(75) Zero-point energy corrections using the harmonic frequencies raise the barrier by only 0.02 kcal/mol for VF_5 and 0.01 kcal/mol for $TaCl_5$.

(76) Ischenko, A. A.; Strand, T. G.; Demidov, A. V.; Spiridonov, V. P. *J. Mol. Struct.* **1978**, *43*, 227.

(77) Petrova, V. N.; Girichev, G. V.; Petrov, V. M.; Goncharuk, V. K. *Zh. Strukt. Khim.* **1985**, *26*, 56.

(78) Demidov, A. V.; Ivanov, A. A.; Ivashkevich, L. S.; Ischenko, A. A.; Spiridonov, V. P.; Almöf, J.; Strand, T. G. *Chem. Phys. Lett.* **1979**, *64*, 528.

(79) (a) Sargent, A. L.; Hall, M. B. *J. Comput. Chem.* **1991**, *12*, 923. (b) Dobbs, K. D.; Hehre, W. J. *Ibid.* **1987**, *8*, 880.

(80) Beattie, I. R.; Ozin, G. A. *J. Chem. Soc. A* **1969**, 1691.

(81) (a) Zolliker, P.; Yon, K.; Fischer, P.; Schefer, J. *Inorg. Chem.* **1985**, *24*, 4177. (b) Zhuang, J.; Hasting, J. M.; Corliss, L. M.; Bau, R.; Wei, C.-Y.; Moyer, R. D. *J. Solid State Chem.* **1981**, *40*, 352.

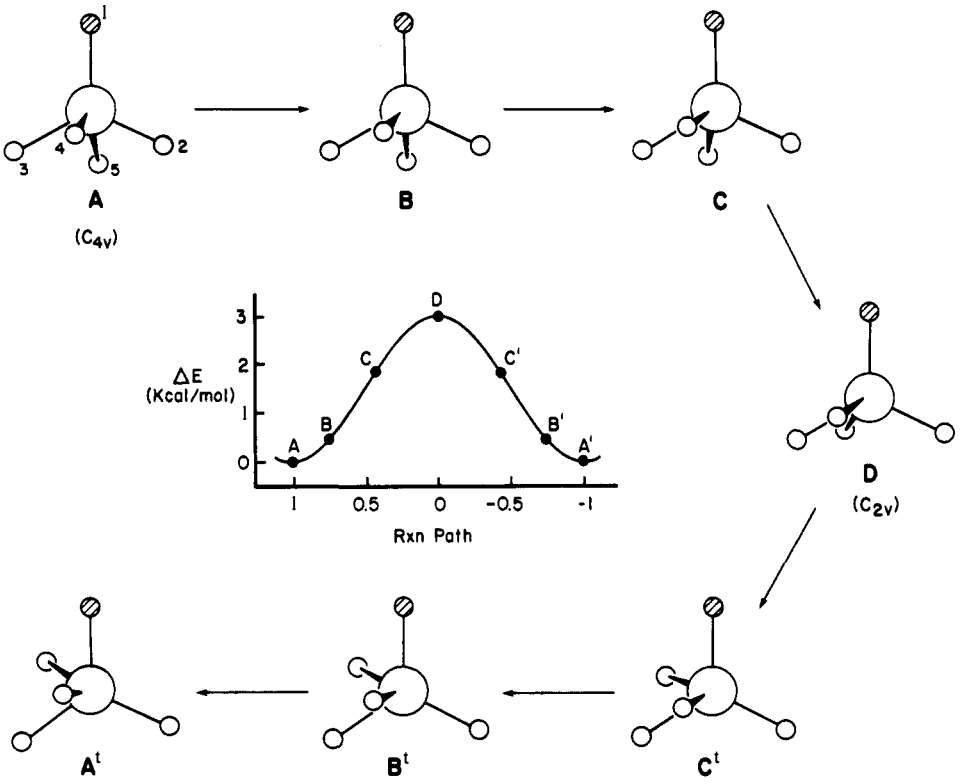

Figure 4. Intrinsic reaction coordinate path for apical–basal exchange in TaH_5 (computed at the HF level). The insert at the center shows the relative energy versus normalized path distance.

we find the D_{3h} structure **33** (Scheme IV) to be 19.5 kcal/mol (at the QCISD(T) level; see Table IV) less stable than the C_{4v} **34**. While C_{4v} is a minimum on the potential energy surface, the D_{3h} structure has imaginary frequencies of a_2'' and e′ symmetry. The a_2'' motion converts D_{3h} to C_{3v}, structure **35**. This isomer has two imaginary frequencies of e symmetry. Inspection of the relative energies in Table IV reveals that an optimization at a higher level of theory may well not yield a stationary point of C_{3v} symmetry.[82]

Careful inspection of the potential energy surface for TaH_5 revealed the existence of another stationary point of C_{2v} symmetry (**35**). Its relative energy lies only 3.1 kcal/mol (QCISD(T) level) higher than C_{4v}, and it has one imaginary frequency of b_2 symmetry. This motion converts the C_{2v} **35** to the C_{4v} global minimum. To confirm this, we computed 15 points between C_{2v} and C_{4v} along the intrinsic reaction coordinate path.[83,84] The results are displayed in Figure 4. Using the numbering system for the hydrogens by structure **A** in this figure, at the C_{4v} geometry the H_2–Ta–H_3 and H_4–Ta–H_5 angles are 124.6°, whereas at the C_{2v} structure they became 120.4° and 130.2°, respectively (the H_3–Ta–H_4 angle is only 65.1°). Thus, the predominant geometrical motion is simply the pivoting of H_4 and H_5 around the axis perpendicular to the plane of the paper in Figure 4. Of course, the same motion exists for H_2 and H_3, where the pivot axis now lies in the plane of the paper. The apical hydrogen H_1 in structure **A** has been shaded. Following the evolution of the reaction path through structure **D** and its mirror image shows that apical–basal exchange has occurred. There have been many proposals[85] of polytopal rearrangement mechanisms in ML_5 complexes, with certainly the most universally accepted one being the Berry process.[74,86] The pivoting mechanism here resembles somewhat the tetrahedral edge transverse, except that the latter begins from the trigonal bipyramid.[85d,87] Here, the trigonal bipyramidal structure, which lies at very high energy, is completely avoided by the pivoting mechanism, which passes through the C_{2v} structure **36**. Notice in Scheme IV that the e′ normal mode on going from D_{3h} (**33**) to C_{2v} (**36**) is precisely identical to, but in an opposite sense, the motion going from D_{3h} (**33**) to C_{4v} (**34**). Thus, the *yz* component of e″ also mixes into and stabilizes a_2'' in Figure 3 upon going to the C_{2v} structure, rendering it more stable than D_{3h}. We should point out that a similar situation exists for d^6 ML_5 species; however, apical–basal exchange here occurs from a C_{2v} distorted trigonal bipyramid where one equatorial–metal–equatorial angle is very acute.[8,70d,f,g] Repeated attempts to locate an analogous stationary point for TaH_5 resulted in collapse to C_{4v}, D_{3h}, and C_{2v} (**35**) structures. The situation we find for VH_5 is very similar to TaH_5 (Table IV). The C_{4v} square pyramid is the ground state, and D_{3h} is 27.4 kcal/mol (QCISD(T) level) higher in energy. A slight difference exists in that the C_{2v} structure **36** (Scheme IV) has two imaginary frequencies of b_2 and b_1 symmetry. Following the b_1 mode produces the C_s **37**. This motion causes the two hydrogens to bend upward by 41.9°. The C_s structure does possess one imaginary frequency of a″ symmetry, which converts it to the C_{4v} ground state. However, its relative energy increases while that for C_{2v} decreases on going to the QCISD and QCISD(T) levels; thus, we expect that the C_{2v} isomer may serve as the transition state for apical–basal exchange at higher levels of theory. For VH_5, we deliberately started geometrical optimizations from two $(\eta^2\text{-}H_2)VH_3$ pseudotetrahedral and three $(\eta^2\text{-}H_2)_2VH$ trigonal planar structures. In all cases, these optimizations simply produced one of the stationary points shown in Scheme IV. Thus, we find for both TaH_5 and VH_5 that

(82) We should point out that very little difference exists between the optimized geometrical parameters at the HF and MP2 levels for the stationary points. However, a stationary point of C_{3v} geometry was not found at the HF level.

(83) (a) Ishida, K.; Morokuma, K.; Konornicki, A. *J. Chem. Phys.* **1977**, *66*, 2153. (b) Schmidt, M. W.; Gordon, M. S.; Dupuis, M. *J. Am. Chem. Soc.* **1985**, *107*, 2585.

(84) The Cartesian coordinates and energies for these structures computed at the HF level are available from the authors upon request.

(85) (a) Ugi, I.; Marquading, D.; Klusacek, H.; Gillespie, P.; Ramirez, F. *Acc. Chem. Res.* **1971**, *4*, 288. (b) Muetterties, E. L. *J. Am. Chem. Soc.* **1969**, *91*, 4115. (c) Jesson, J. P.; Meakin, P. *Ibid.* **1974**, *96*, 5760. (d) Meakin, P.; Muetterties, E. L.; Jesson, J. P. *Ibid.* **1972**, *94*, 5271.

(86) For example, collection of the crystal structures for 18-electron ML_5 complexes sample a reaction path that follows Berry pseudorotation: Muetterties, E. L.; Guggenberger, L. J. *J. Am. Chem. Soc.* **1974**, *96*, 1748.

(87) (a) Muetterties, E. L.; Hirsekorn, I. J. *J. Am. Chem. Soc.* **1973**, *95*, 5419. (b) Miller, J. S.; Caulton, K. G. *Inorg. Chem.* **1975**, *14*, 2296.

Scheme V

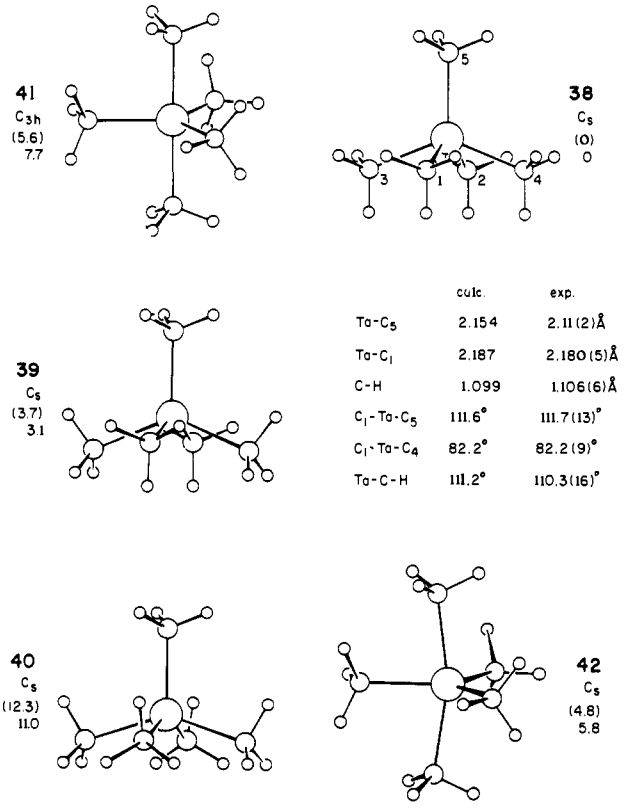

the D_{3h} geometry is a higher-order saddle point. The ground-state geometry for both is C_{4v}, and a low-energy path exists for apical–basal exchange which avoids the trigonal bipyramid. Replacement of the hydrogens with methyl groups will not alter the electronic situation. The steric bulk of a methyl group is certainly larger, however, than that of a hydrogen, and consequently the energy differences between the VSEPR-mandated trigonal bipyramid and the square pyramid or certainly the C_{2v} structure analogous to **36** are expected to be smaller. With this in mind, we proceed to $TaMe_5$.

$TaMe_5$ has been known since 1974[88] and was assumed to be a trigonal bipyramid. Very recently, Haaland and co-workers[89] investigated its structure by electron diffraction and found $TaMe_5$ to be a square pyramid. Our HF optimizations are reported in Scheme V,[90] where relative energies in kcal/mol at the HF level are listed in parentheses and those from single point MP2 calculations are listed below them. Starting with the square pyramid, three rotomers, **38**–**40**, were considered and optimized within C_s symmetry. Of these, **38** is the lowest and corresponds to the structural model used by Haaland and co-workers.[89] The averaged theoretical[91] and experimental details are given below the structure. The agreement between theory and experiment is excellent. We feel that the higher energies associated with **39** and **40** are primarily steric in origin. Both structures contain more eclipsing H–C–Ta–C interactions. Furthermore, the nonbonded H···H distances between basal methyl groups in **40** are considerably shorter than in the other rotomers. Another rotomer where one basal methyl group was oriented so that only one C–H bond eclipsed the Ta–C_{apical} bond was optimized in C_s symmetry. Its HF relative energy was found to be 3.7 kcal/mol higher than **38**.

Critical to our discussion, we find that trigonal bipyramid **41**, with C_{3h} symmetry, lies 7.7 kcal/mol higher in energy (at the MP2 level) than **38**. Other methyl group orientations were tried for a trigonal bipyramid; however, these either were computed to be at higher energies or collapsed to **41**. The ^{13}C NMR of $TaMe_5$ consists of one sharp resonance down to −120 °C.[89] This implies that $\Delta G^{\ddagger} < \sim 7$ kcal/mol for apical–basal exchange. Given our findings for the exchange pathway associated with TaH_5 and VH_5, special care was taken to search for an analogous transition state in $TaMe_5$. This included trials with four different methyl group orientations and a scan of the potential energy surface in two dimensions. In the pivoting mechanism, two trans basal methyl groups, for example C_1 and C_2 in **38**, rotate around an axis perpendicular to the molecular mirror plane until they approximately eclipse the Ta–C_3 (or Ta–C_4) bond. This motion can be conveniently described by changes in one dihedral angle. This dihedral angle, along with the C_1–Ta–C_3 (C_2–Ta–C_3) bond angle, was used to construct the two-dimensional surface and to crudely locate a saddle point. These two variables were then frozen, and the remaining internal coordinates were optimized in C_s symmetry. Finally, the force constants associated with the two variables were numerically computed, and the full transition state optimization produced structure **42**. The eigenvector associated with the one negative eigenvalue in the Hessian matrix was almost exclusively associated with the aforementioned dihedral angle. Structure **42** contains basically the same methyl group orientation as in the trigonal bipyramid **41**. However, the two axial groups are bent 8.9° from their idealized positions *toward* one equatorial methyl group, as in the C_{2v} geometry of TaH_5 (**36**, Scheme IV). The MP2 energy of **42** was 2.1 kcal/mol more stable than that of **41** (5.8 kcal/mol above the ground state **38**). While we have not computed the frequencies associated with **42**, nor have we followed the intrinsic reaction coordinate from **38** to **42**, nonetheless, we believe that the pivoting mechanism represents a viable option for apical–basal exchange in $TaMe_5$.

Conclusions and Extensions

We have shown that the structures anticipated by the VSEPR rules for d^0 ML_6 and ML_5 complexes (namely the octahedron and the trigonal bipyramid, respectively) lie at high relative energies when certain conditions are met. The M–L bond should be reasonably covalent, and L must be a strong σ-donor, sterically not demanding, and have little π-donating capabilities. The optimal structure for CrH_6 appears most likely to be an $(\eta^2\text{-}H_2)_3Cr$ species, although a C_{3v} distorted octahedron or trigonal prism may well represent lower-energy structures at a higher computational level. For WH_6 the C_{3v} distorted trigonal prism or a C_{5v} pentagonal prism is found to be the ground state. All of the structures with C_{3v} symmetry can be directly predicted by use of the second-order Jahn–Teller model in that all three members of the low-lying, empty t_{2g} set mix into and stabilize the three members of the high-lying, filled t_{1u} set. Maximal involvement of the d orbitals at the transition metal is thus attained. The C_{5v} pentagonal prism represents another solution to maximize d orbital mixing. Since the methyl groups are considerably bulkier than hydrogens, the distortion in WMe_6 stops at the trigonal prism and the optimal structure is in close agreement with experiment. In TaH_5, VH_5, and $TaMe_5$ at the trigonal bipyramidal geometry, there is a small energy gap between the empty e″ set and a filled a_2'' orbital. The Jahn–Teller method predicts that an e′ motion will be stabilizing. This motion in one direction produces a square pyramid, which is the ground state for all three species. An e′ motion in the opposite sense (toward one equatorial bond) produces a C_{2v} structure, which serves as the transition state for apical–basal exchange. The reaction path on going from the square pyramid to the C_{2v} transition state is a novel pivoting process of two trans basal ligands. This motion completely avoids the higher-energy trigonal bipyramidal structure. The optimal structure for $TaMe_5$ is in close agreement with experiment. The energy gains on going from the VSEPR to the optimal structure are much larger for the d^0 ML_6 cases than that found for d^0 ML_5. In ML_6, two or all three components of the empty t_{2g} set can mix into the t_{1u} set.

(88) (a) Schrock, R. R.; Meakin, P. *J. Am. Chem. Soc.* **1974**, *96*, 5288. (b) Schrock, R. R. *J. Organomet. Chem.* **1976**, *122*, 209.

(89) Haaland, A.; Hammel, A.; Rypdal, K.; Verne, H. P.; Volden, H. V.; Pulham, C.; Brunvoll, J.; Weidlein, J.; Greune, M. *Angew. Chem.* **1992**, *104*, 1534.

(90) A preliminary account of D_{3h} and C_{4v} structures of TaH_5 and $TaMe_5$ is given in Albright, T. A.; Tang, H. *Angew. Chem.* **1992**, *104*, 1532.

(91) The individual bond lengths and C–Ta–C and Ta–C–H bond angles differ by not more than 0.005 Å, 0.1°, and 0.8°, respectively, in the C_s optimized structure.

However, in ML_5 only one member of e'' mixes into the a_2'' HOMO. All d^0 MX_6 and MX_5 molecules studied here possess the VSEPR-mandated structures; namely, CrF_6 and WF_6 are found to be octahedral and VF_5 along with $TaCl_5$ are trigonal bipyramids. The situation for other ML_n complexes can be easily obtained in a qualitative fashion.

The valence orbitals of a d^0 MH_4 complex are presented on the right side of Figure 3. At the tetrahedral geometry there are again two empty d metal nonbonding orbitals. However, the t_2 HOMO already contains maximal d character. Thus, it is not surprising that TiH_4, which is a known compound,[92] has been found to be a local minimum (and in all likelihood the global minimum) at the tetrahedral geometry.[10,93] For a d^0 ML_2 system at the $D_{\infty h}$ geometry, the filled σ_u^+ orbital **43** has exclusively p character at the metal. One component of π_g, shown in **44**, will strongly mix into **43** upon bending to a C_{2v} structure. Thus, even in the highly ionic SrH_2 and BaH_2 molecules, bent rather than linear geometries are found.[9b] Furthermore, the calculated bending force constant varies inversely with the percentage of metal d hybridization for MX_2 molecules where M = Sr and Ba.[9a] The HOMO and LUMO for a trigonal planar d^0 MH_3 molecule are e' and e'', respectively (precisely analogous to e' and e'' for MH_5 on the left side of Figure 3). Although the e' set contains d character at the metal, upon pyramidalization e'' will mix into e', thus increasing the metal d hybridization. Jolly and Marynick[10] have found that ScH_3, TiH_3^+, and $TiMe_3^+$ all prefer pyramidal over planar structures at the HF level. We suspect that this will also be true when allowance is made for electron correlation.

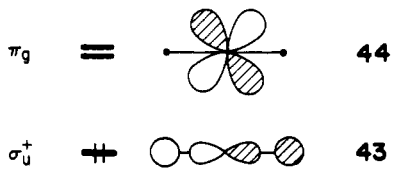

(92) (a) Breisacher, A.; Siegel, B. *J. Am. Chem. Soc.* **1963**, *85*, 1705. (b) Xiao, Z. L.; Hauge, R. H.; Margrave, J. L. *J. Phys. Chem.* **1991**, *95*, 2696.
(93) Thomas, J. R.; Quelch, G. E.; Seidl, E. T.; Schaeffer, H. F., III *J. Chem. Phys.* **1992**, *96*, 6857.

Acknowledgment. We wish to thank Drs. Arne Haaland, Jeremy Burdett, Odile Eisenstein, Oleg Charkin, Colin Marsden, Dennis Marynick, Fritz Schaeffer, and Monte Pettitt for many stimulating discussions. We gratefully acknowledge support from the Robert A. Welch Foundation, the donors of the Petroleum Research Fund as administered by the American Chemical Society, and the University of Houston's President's Research Enhancement Fund, and thanks are due to the National Science Foundation for a generous allocation of computer time at the Pittsburgh Supercomputing Center.

Supplementary Material Available: Coordinates (in Z-matrix form), total energies, and harmonic frequencies for **1-42** (45 pages). Ordering information is given on any current masthead page.

Interlayer Communication in Some Two-Dimensional Materials

Seeyearl Seong, Kyeong-Ae Yee, and Thomas A. Albright*

Contribution from the Department of Chemistry and Texas Center for Superconductivity, University of Houston, Houston, Texas 77204-5641. *Received September 18, 1992*

Abstract: Tight binding calculations with an extended Hückel Hamiltonian were used to probe interlayer bonding in four representative compounds. In V_2O_5, a straightforward interaction exists between the apical oxygen lone pairs and empty z^2 orbitals on vanadium in adjacent layers. There exists no covalent bonding between $Bi_2O_2^{2+}$ and WO_4^{2-} layers in Bi_2WO_6 at the prototype geometry. However, when the metal octahedra are tilted and the perovskite layer is shifted in its registry, two relatively strong bonds form between the out-of-plane oxygen atoms in the perovskite layer and bismuth. Here the interaction transfers electron density from the oxygen lone pairs to empty Bi–O σ^* orbitals. This, in turn, creates structural deformations within the $Bi_2O_2^{2+}$ layer. For $LiBiPd_2O_4$, we find covalent interaction between bismuth and palladium. Yet this does not appear to be the case in the topologically analogous $Pd_3P_2S_8$ structure. The reasons for the differences in covalent interaction are discussed in detail.

Introduction

From a geometrical point of view, layered or lamellar compounds[1] are inherently two-dimensional. A popular definition[1a] requires that they consist of electrically neutral layers held together only by van der Waals forces. Thus, layered compounds are easily cleaved, and the freshly exposed surfaces are relatively inert. Layer-type compounds have been extensively studied[1] in recent years, not only for their use as lubricants, etc., but also because of their highly anisotropic properties. Graphite and its fluorinated analog are perhaps the most well-known examples. In most compounds, the top and bottom layers of the "sandwiches" consist of anions only or, in some rare cases, of cations only.[1a,b] An interesting feature of many of these compounds is that their quasi-three-dimensional character can be gradually weakened or reinforced by intercalation with metal or organic radicals. Most frequently, electrostatic forces exist between the layer and the intercalate.

Trinquier and Hoffmann have suggested that weak covalent interlayer bonding exists between Pb atoms in adjacent layers in α- and β-PbO.[2] Likewise, weak interactions between Te atoms in certain MTe_2 phases have been found by Canadell, Whangbo, and co-workers.[3] It is our contention that this is a more general phenomena and that in many cases the remnants of covalent bonding can be found in layered compounds and intercalated

(1) (a) Hulliger, F. In *Structural Chemistry of Layer-Type Phases*; Levy, F., Ed.; D. Reidel: Dordrecht, 1976. (b) Bronger, W. In *Crystallography and Crystal Chemistry of Materials with Layered Structures*; Levy, F., Ed.; D. Reidel: Dordrecht, 1976. (c) Rouxel, J. In *Intercalated Layer Materials*; Levy, F., Ed.; D. Reidel: Dordrecht, 1979. (d) Grasso, V. *Electronic Structure and Electronic Transitions in Layered Materials*; D. Reidel: Dordrecht, 1986.

(2) Trinquier, G.; Hoffmann, R. *J. Phys. Chem.* **1984**, *88*, 6696.
(3) Canadell, E.; Jobic, S.; Brec, R.; Rouxel, J.; Whangbo, M.-H. *J. Solid State Chem.* **1992**, *99*, 189 and references therein.

0002-7863/93/1515-1981$04.00/0